

CALCULATED ELASTIC SCATTERING CROSS SECTIONS FOR COO-1328-12
THE $\text{Li}^+\text{-He}$ SYSTEM*

by

G. G. Weber and R. B. Bernstein

Theoretical Chemistry Institute, University of Wisconsin

Madison, Wisconsin 53706

ABSTRACT

29398

Calculations of the energy dependence of the total (and differential) elastic scattering cross sections for the $\text{Li}^+\text{-He}$ system have been carried out for a number of assumed interaction potentials (from the literature). All of these are known to yield good fits to existing mobility data, sensitive primarily to the long-range r^{-4} term in the potential. The present results show that the total quantum cross sections (as well as the angular distributions) are quite sensitive to the potential also at short range (e.g. $r < 4\text{\AA}$), even at low collision energies ($E < 1\text{eV}$). In particular, the behavior of the extrema in the total cross sections offers a means of discrimination among the potentials.

Author

- - - - -
* Work supported by the National Aeronautics and Space Administration, Grant NsG-275-62 and the U.S.A.E.C., Div. of Research, Contract AT(11-1)-1328.

Available to NASA Offices and
Users

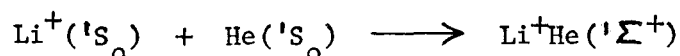
Introduction

Although there have been a number¹ of semiempirical and quantum theoretical investigations² of the elastic scattering of ions by atoms (or simple molecules), they have generally been concerned with the interpretation of ion mobilities and diffusion coefficients in the thermal range. It appears that there has been little effort directed toward an examination of the quantum effects in the total and differential beam scattering cross sections and their possible usefulness in elucidating the interaction potential.

The present paper reports a quantal computation of the total and differential cross sections for the Li^+ - He system in its ground state, using for the calculation of the phase shifts the Jeffreys-WKBL (JWKBL) and the Jeffreys-Born (JB) approximations under conditions of demonstrable reliability. It will be seen that the quantum effects for the ion-atom system have many qualitative features in common with those obtained for the atom-atom case³ with the principal differences arising from the long-range (r^{-4}) attractive part of the potential. The extrema in the total cross-sections (i.e., in the ion-atom impact spectra) as a function of velocity offer a means of discrimination among the potentials via low energy beam scattering measurements.

Procedures

Calculations have been carried out for seven ($j = 1, \dots, 7$) interaction potentials proposed in the literature⁴⁻⁶ for the Li^+ - He system corresponding to



Each potential is plausible from the viewpoint of a reasonable long range behavior (i.e. $V(r) \sim -\frac{C^{(4)}}{r^4}$, with $C^{(4)} = \alpha/2$, where α is the He polarizability; all quantities in a.u.), which produces a fairly satisfactory fit to the experimental mobility data. Six of them may be written with an exponential repulsion term:

$$V_j(r) = D_4 \exp(-D_5 r) - D_2 r^{-6} - D_3 r^{-4} (1 + D_6 r^{-2}) \quad (1)$$

while the other (the semiempirical potential, $j = 4$) is most simply written

$$V_4(r) = D_1 r^{-12} - D_2 r^{-6} - D_3 r^{-4} \quad (2)$$

Table I lists the relevant details (references, constants, quantities describing the potential shapes, and comments). The potentials are plotted in Fig. 1.

Well known methods were employed for the computation of the phase shifts $[\eta_e]$ and the total $[Q]$ as well as differential $[I(\theta)]$ elastic cross sections as a function of relative velocity (v) or collision energy (E), as outlined below.

Phase shifts were computed by the JWKBL⁷ or by the JB⁸ approximation in the regions where these methods are applicable. A number of phase shifts were checked by direct numerical integration⁹ (RKG method) of the radial equation. A few of these checks are presented in Table II. The computations were carried

out with a CDC1604 computer at the University of Wisconsin Computing Center.

The calculations employed a reduced notation; thus the JWKB phase shift is written:

$$\eta_{\text{JWKB}} = A \left\{ \frac{\pi\beta}{2} - x_0 - \int_{x_0}^{\infty} [f(x)^{1/2} - 1] dx \right\} \quad (3)$$

where $x \equiv r/a_0$, $A \equiv ka_0$, $\beta \equiv (\ell + 1/2)/A$,
 $f(x) = 1 - \frac{V(x)}{E} - \beta^2 x^{-2}$, $E = \frac{1}{2}\mu v^2 = \hbar^2 k^2/2\mu$

and $x_0 \equiv r_0/a_0$ is the outermost zero of $f(x)$ (i.e., r_0 is the classical turning point). Eq. 3 is converted to a more practical form for numerical computation:

$$\eta_{\text{JWKB}} = A \left\{ \frac{\pi\beta}{2} - 1/\gamma_0 + [1 - (1 - \beta^2 z^2)^{1/2}] \cdot z^{-1} \right. \\ \left. - \beta^2 z (1 + \beta^2 z^2/6) + I(z, \gamma_0) \right\} \quad (4)$$

where

$$I(z, \gamma_0) = \int_z^{\gamma_0} [f(y)^{1/2} - 1] y^{-2} dy$$

$y \equiv 1/x$, $\gamma_0 = a_0/r_0$. Here z is a small constant ($0 < z < .01$; typically $z = .005$) introduced to aid in the computation of the part of the integral for which the integrand is nearly singular. $I(z, \gamma_0)$ is evaluated by Gaussian quadrature.

The JB phase shifts are given by:

$$\eta_{JB}^{(4,6)} = \frac{\pi}{8} \cdot \frac{C^{(4)} BA^2}{(\ell + 1/2)^3} + \frac{3\pi}{16} \cdot \frac{C^{(6)} BA^4}{(\ell + 1/2)^5} \quad (5)$$

where $C^{(4)}$ and $C^{(6)}$ are, respectively, the coefficients of the r^{-4} and r^{-6} terms in the potentials; $B \equiv 2\mu\epsilon a_0^2/\hbar^2$, where ϵ is the depth of the potential well.

The program for the phase shifts computes η_e by the JWKB method (Eq. 4) for each ℓ (at the specified v) until $\ell \geq \ell^*$ (well beyond ℓ_r , the rainbow¹⁰ angular momentum). In this region η is decreasing monotonically with increasing ℓ ; also $\left| \frac{d\eta}{d\ell} \right|$ is decreasing monotonically. The criterion for use of the JB approximation is

$$|\eta_{JWKB}(\ell^*) - \eta_{JB}(\ell^*)| \leq .01$$

For $\ell \geq \ell^*$ the program calculates only η_{JB} . In every case the calculations terminate when $\eta_e \leq .01$ (and $\ell \geq \ell^*$).

Sample comparisons of JWKB, JB, and RKG phases are presented below.

From the phase shifts the total (Q) and differential $[I(\theta)]$ elastic cross sections are calculated according to well known procedures^{7a,9}. In addition a "reduced" differential cross section¹¹ is computed:

$$\rho^*(\theta) = I(\theta) \cdot \left\{ \frac{8}{(3\pi)^{1/2}} \cdot \left[\frac{E}{C^{(4)}} \right]^{1/2} \cdot \theta^{3/2} \sin \theta \right\} \quad (6)$$

The function $\rho^*(\theta)$ approaches unity in the classical limit at small angles (e.g. $\theta < 30^\circ$).

Due to the known unreliability of the JWKB approximation for energies sufficiently low such that classical orbiting is possible, the calculations were restricted to $E > E_{\text{crit}}$ (or $A > A_{\text{min}}$). Here $E_{\text{cr.}} = V(x_{\text{cr.}})$ can be evaluated from the relation:

$$x_{\text{cr.}} V''(x_{\text{cr.}}) + 3 V'(x_{\text{cr.}}) = 0 \quad (7)$$

The upper limit of E was set by the unphysical maxima, V_{max} , occurring at small r for all potentials except 4. Appendix I gives further details.

Results

A. Phase Shifts

The actual phase shifts used in the cross section calculations are, of course, too numerous to list. However, Table II presents a sample of check calculations of phase shifts carried out by the different procedures described. The accuracy of the phase shifts over the entire range of the calculations is believed to be $\pm .01$. Table III shows a comparison of certain high-order phases for several potentials at the same A (i.e. same velocity or $E_{\text{kin.}}$). Agreement is satisfactory, in view of the wide range of the potential parameters ξ , R_m , B . This shows the dominant influence of the attractive terms (at large ℓ) and the consistency of the calculations.

B. Total Cross Sections

Fig. 2 shows a log-log plot of $Q(v)$ for potentials 4 and 7. The average low energy behavior is almost entirely governed by the long-range part (r^{-4}) of the potential. The (monotonic) overall velocity dependence is well described by the Schiff-Landau-Lifshitz (SLL) formula:^{11,12}

$$Q_{SLL}^{(4)} = 11.373 \left[C^{(4)} / \hbar v \right]^{2/3} \quad (8)$$

In the low-velocity region the oscillatory behavior (extrema in $Q(v)$, Fig. 2; shown as $\Delta Q/Q$ vs. $1/v$ in Fig. 3) is qualitatively the same as in atom-atom scattering.¹³ The extrema will be further discussed below.

For potential 4 with its r^{-12} repulsive term the high-velocity behavior is expected to approach the form

$$Q_{SLL}^{(12)} = 6.584 \left[C^{(12)} / \hbar v \right]^{2/11} \quad (9)$$

with the difference between Q and $Q_{SLL}^{(12)}$ slowly approaching zero as $v \rightarrow \infty$. Table IV summarizes the high-velocity results which allow for an extrapolation of the fractional difference $(Q_{SLL} - Q)/Q_{SLL}$ to the limit $1/A = 0$. The result is indeed zero within the uncertainty of the extrapolation ($\approx 0.2\%$). For the highest energies the calculation of a single Q required some 11,000 JWKB integrations and an additional 4000 JB-phases; the result of the extrapolation test shows that there is very little

cumulative error in the cross section computations.

The low velocity results (Fig. 3) show a nearly symmetrical oscillation about $Q_{SLL}^{(4)}(v)$, as expected.¹¹⁻¹⁴ Fig. 4 summarizes all the total cross section calculations (ion-atom impact spectra¹¹⁻¹³) in the form of graphs of the "apparent" $C^{(4)}$ vs. $1/v$. The $C_{app}^{(4)}$ values are found to oscillate about the theoretical (assumed) value for $C^{(4)}$, namely 2.34×10^{-44} erg cm⁴, indicated by a mark on the ordinate scale. The undulatory behavior is, of course, different for each potential, offering a possible means of discrimination.

Fig. 5 shows for a broad region of velocities the ion-atom impact spectrum (for Potential 1) in which the extrema are indexed according to the method of Refs. 13b,c. The initial slopes $S_o = \left[\frac{dN}{d(1/v)} \right]_{1/v = 0}$ of such plots of N vs $1/v$ are recorded in Table V.

For a series of potentials with the same functional form, differing only in the numerical values of the parameters, such slopes should be a linear function of the product $\epsilon \cdot r_m$ (or $\epsilon \sigma$, where σ is the usual zero of the potential). Not all the potentials have the required similarity; nevertheless S_o is found to be an almost linear function of $\epsilon \sigma$ (and ϵr_m). By fitting the results for potentials 1-7, it is possible to estimate from any given S_o a value for $\epsilon \sigma$, say $(\epsilon \sigma)'$, which is quite close to the known value.

Table V summarizes the results, indicating the degree of correlation. This suggests that an estimate of the $\epsilon \sigma$ product (considerably better than $\pm 5\%$) can be made directly from an observed extrema-pattern with no further analysis.

C. Differential Cross Sections.

Fig. 6 shows a typical result for $I(\theta)$, while Fig. 7 is a presentation of the same calculations in terms of $p^*(\theta)$. The angular scattering pattern (with the diffraction maxima showing both single and double periodicity) are, of course, very sensitive to the potential function.^{10,11} Table VI presents samples of the computed patterns, indicating something of the periodicity and amplitude of the quantum interferences to be expected from high-resolution, low energy beam scattering measurements.

Acknowledgment

The authors wish to thank Mrs. Carol Monash for her skillful assistance in the programming of the computations.

TABLE I

Interaction Potentials for the $\text{Li}^+ - \text{He}$ System. (All quantities in a.u.)

V_j Ref.No.	D_1	D_2	D_3	D_4	D_5	D_6	\mathcal{E}	R_m	σ	B
1	4	0	.6850	44.38	3.044	0	.00392	3.18	2.65	36.45
2	4	1.922	.6905	44.38	3.044	0	.00649	2.88	2.37	60.29
3	4	1.922	.6905	3.82	1.800	0	.000785	4.72	3.85	6.920
4	4	51680.	.6905	2.75	2.75	-	.00174	4.195	3.67	16.18
5	5	-	.6950	37.10	3.120	0	.01046	2.50	1.98	135.2
6	4	-	.6905	44.38	3.044	1.590	.00883	2.69	2.17	82.00
7	6	-	.6950	37.10	2.750	0	.002296	3.68	3.08	21.33

Comments on potentials $j = 1, \dots, 7$:

- (1) First-order exchange terms evaluated "exactly".
- (2) Similar to 1, but with added r^{-6} term.
- (3) Approximation of second-order exchange terms.
- (4) Semi-empirical fitted to mobility (D_2 also contains the quadrupole-quadrupole forces).
- (5) First-order exchange terms calculated approximately.
- (6) Similar to 2, but better evaluation of inductive energy.
- (7) Semi-empirical, fitted to mobility.

TABLE II

Sample calculations of phase shifts by the different proceduresA. (1) Potential 4, $A = 21.236$ ($v = 1.00 \times 10^6$ cm/sec, $E = 1.32$ eV)

l	η_{RKG}	η_{JWKBL}	$\eta_{JB}^{(4)}$	$\eta_{JB}^{(4,6)}$
0	-64.138	-64.131	-	-
10	-49.377	-49.369	-	-
50	-8.240	-8.231	-	-
150	+0.354	+0.355	-	-
153	.315	.334	.314	-
160	.290	.291	.275	.290

(2) Potential 7, $A = 5.00$ ($v = 2.35 \times 10^5$ cm/sec, $E = 0.0732$ eV)

l	η_{RKG}	η_{JWKBL}
0	-9.762	-9.752

B. Change-over from JWKBL to JB approximation at $l = l^*$

Potential 4

A	E(eV)	l^*	η_{JWKBL}	$\eta_{JB}^{(4,6)}$
50	7.32	275	0.325	0.332
100	29.29	503	.211	.221
300	263.6	1368	.091 ₅	.101 ₄
600	1054.	2568	.052 ₄	.062 ₄

TABLE III

Comparison of high order phases for several potentials

$$A = 5 \quad (v = 2.35 \times 10^5 \text{ cm/sec}, \quad E = 0.0732 \text{ eV})$$

η_e

l	V1	V3	V7
130	0.0285	0.0274	0.0289
140	.0231	.0222	.0235
150	.0192	.0185	.0195
160	.0164	.0158	.0167

TABLE IV

Extrapolation of $\Delta Q/Q_{SLL}$ to $1/v \rightarrow 0$

A	1/A	Q(v) a.u.	$Q_{SLL}^{(12)}$ a.u.	$(Q_{SLL} - Q)/Q_{SLL}$
500	0.0020	59.0	63.7 ₅	0.075
1000	0.0010	53.2 ₅	56.2	.052
2000	0.0005	47.9	49.5	.033
3000	0.00033	44.9	46.0	.024
∞	0	0	0	.001 ₅ *

* Extrapolation using Aitken procedure.

TABLE V

Initial slopes $S_0 = \left(\frac{dN}{d(1/v)} \right)_{\frac{1}{v} = 0}$ and their correlation with $\epsilon\sigma$

Potential	$\epsilon\sigma$ (a.u.)	$10^{-6} \times S$ (cm/sec)	Ratio $10^8 \times (\epsilon\sigma/S)$
1	0.010388	0.9667	1.075
2	.01494	1.407	1.062
3	.00289	.2779	1.040
4	.00550	.5019	1.096
5	.02030	1.816	1.118
6	.01930	1.738	1.110
7	.00699	.6437	1.086

Avg. $1.08_4 \pm 0.02$

Table VI

Angular Distributions $\rho^*(\theta)$

Potential 7, A=5.00 E=0.073 eV		Potential 2, A=5.00 E=0.073 eV		Potential 5, A=10.0 E=0.293 eV	
θ (deg.)	Maximum Minimum	θ (deg.)	Maximum Minimum	θ (deg.)	Maximum Minimum
1.60	1.295	1.40	1.615	1.30	1.403
3.70	.5459	2.55 } 2.85 }	.945	2.15	1.046
6.10	1.066	.9667		2.70	1.252
7.75	.6497	3.55	.796	4.25	.796
12.15	1.971	4.25	.939	5.05	1.149
14.55	.8361	4.60	.922	6.90 } 7.20 } 7.50 }	.480
17.45 } 17.60 }	1.854	5.30	1.078	.491	.480
18.45 }	1.853	7.00	.355		
21.80	1.892	9.15	1.369	9.45	1.478
24.95	.9679	10.90	.718	11.15	.863
27.90	.0054	13.05	2.400	13.20	2.238
		15.35	.763	15.90	.470
		17.90	1.876	17.25	1.085
		20.20	.106	19.60	.0399
		22.20	.960	21.55	1.259
		24.20	.00066	23.60	.381
		26.70	1.427	26.40	3.069
		28.70	.245	28.65	.851

Appendix I

All potentials (except V4) possess unphysical maxima (V_{\max}) such that for $A > A_{\max}$ (i.e., $E > E_{\max}$) no calculations are possible. For every potential (including V4) the onset of the orbiting phenomenon at low energies defines an A_{\min} , below which the JWKB approximation cannot be reliable. Both extremes are listed in Table VII.

TABLE VII

Highest and lowest energy consistent with the potential

j	A_{\max}	A_{\min}	E_{\max} (eV)	E_{\min} (eV)
1	149.0	3.70	66.	0.04
2	44.0	4.84	5.9	.07
3	16.65	1.59	.79	.007
4	no A_{\max} *	2.82	no E_{\max} *	.03
5	22.43	6.95	1.5	.14
6	23.63	5.64	1.6	.09
7	153.48	2.93	66.	.03

* The highest velocity-parameter evaluated here was $A = 3000$, which corresponds to 8.58 keV.

Appendix II

Tabulated below are interpolated "best values" of v_N , i.e. the velocities corresponding to the extrema in the computed ion-atom impact spectra (C_{app} vs. $1/v$) derived from the total cross sections. The error in the interpolation is believed to be less than 1%. The range of extrema in each case is limited by the velocity range of the calculation, i.e. $A_{min} \leq A \leq A_{max}$. (Table VIII).

TABLE VIII

Velocities corresponding to extrema of the impact spectrum

Potential	N	$10^{-5} \times v_N$ (cm/sec)	E_N (eV)
1	1	15.47	3.16
	1.5	8.20	0.888
	2	5.46	.394
	2.5	3.94	.205
	3	2.80	.103
2	1.5	12.51	2.07
	2	8.47	0.947
	2.5	6.21	.509
	3	4.78	.302

TABLE VIII (cont'd)

Potential	N	$10^{-5} \times v_N$ (cm/sec)	E_N (eV)
3	1	4.45	0.261
	1.5	2.30	.070
4	1	8.03	.852
	1.5	4.28	.242
	2	2.79	.103
	2.5	1.93	.049
5	2.5	8.55	.965
	3	7.10	.666
	3.5	5.99	.474
	4	4.89	.316
6	2.5	8.18	.884
	3	6.40	.541
	3.5	3.31	.145
7	1	10.30	1.401
	1.5	5.19	0.356
	2	3.52	.164

List of Footnotes

1. For reviews, see (a) E. A. Mason and H. W. Schamp, Jr. *Ann. Physics (N.Y.)* 4, 233 (1958); (b) A. Dalgarno, in Atomic and Molecular Collision Processes, ed. by D. R. Bates, Academic Press, N.Y. 1962, p. 643; (c) E. A. Mason and J. T. Vanderslice, *ibid.*, p. 663.
2. (a) S. Geltman, *Phys. Rev.* 90, 808 (1953); (b) A. Dalgarno, M. R. C. McDowell and A. Williams, *Phil. Trans. Roy. Soc. (London)* A250, 411 (1958).
3. For reviews, see (a) R. B. Bernstein, *Science* 144, 141 (1964); (b) R. B. Bernstein, in Atomic Collision Processes, ed. by M. R. C. McDowell, North-Holland Publ. Co., 1964, p. 895.
4. E. A. Mason, H. W. Schamp, Jr. and J. T. Vanderslice, *Phys. Rev.* 112, 445 (1958).
5. R. E. Meyerott, *Phys. Rev.* 66, 242 (1944).
6. Ref. 2b
7. See, for example, (a) N. F. Mott and H. S. W. Massey, Theory of Atomic Collisions, Clarendon Press, Oxford, 3rd Ed. (in press);
Ed. by
(b) B. S. Jeffreys, in Quantum Theory I./D. R. Bates, Academic Press, N.Y. 1961, p. 229 ; (c) T. Wu and T. Ohmura, Quantum Theory of Scattering, Prentice-Hall, N.Y. 1962; (d) R. P. Marchi and C. R. Mueller, *J. Chem. Phys.* 38, 740 (1963); also, (e) R. J. Munn, E. A. Mason and F. J. Smith, *J. Chem. Phys.* (to be published).
8. (a) H. S. W. Massey and C. B. O. Mohr, *Proc. Roy. Soc. (London)* A144, 188 (1934); (b) H. S. W. Massey and R. A. Smith, *ibid.* A142, 142 (1933).

List of Footnotes (cont'd)

9. R. B. Bernstein, J. Chem. Phys. 33, 795 (1960).
10. K. W. Ford and J. A. Wheeler, Ann. Phys. (N.Y.) 7, 259 (1959).
11. R. B. Bernstein, in Advances in Chemical Physics, VIII, "Molecular Beams", Ed. by I. Prigogine and J. Ross, J. Wiley and Sons, N.Y. 1965.
12. R. B. Bernstein and K. H. Kramer, J. Chem. Phys. 38, 2507 (1963).
13. R. B. Bernstein, J. Chem. Phys. (a) 34, 361 (1961); (b) 37, 1880 (1962); (c) 38, 2599 (1963).
14. R. Düren and H. Pauly, Z. f. Phys. 175, 227 (1963); 177, 146 (1964).

Legend for Figures

1. Seven potentials from the literature proposed for the $\text{Li}^+\text{-He}$ interaction.
2. Total cross sections Q vs. velocity v (log-log presentation), for two potentials with $Q_{\text{SLL}}^{(4)}$ - average for low velocities and $Q_{\text{SLL}}^{(12)}$ - limit for high velocities. $Q_{\text{SLL}}^{(4)}$ and $Q_{\text{SLL}}^{(12)}$ are shown as dashed lines; the solid curve from $A = 1$ to 1000 refers to potential 4, while the other curve with primed indices is for V7.
3. Relative deviation of Q , i.e., $\Delta Q/Q_{\text{SLL}}$ vs. $1/v$ for V4.
4. Relative deviation of C_{app} for all potentials, i.e. C_{app} vs. $1/v$. The A_{max} is indicated (except for V4 where there is none).
5. C_{app} for V1, indicating the extrema of C_{app} ($1/v$).
Below: Index N of the extremum vs. $1/v_N$, showing the "initial slope".
6. Example of an angular distribution: the differential cross section $I(\theta)$.
7. Example of an angular distribution: the reduced differential cross section $\rho^*(\theta)$. Note the superposition of two different periods.

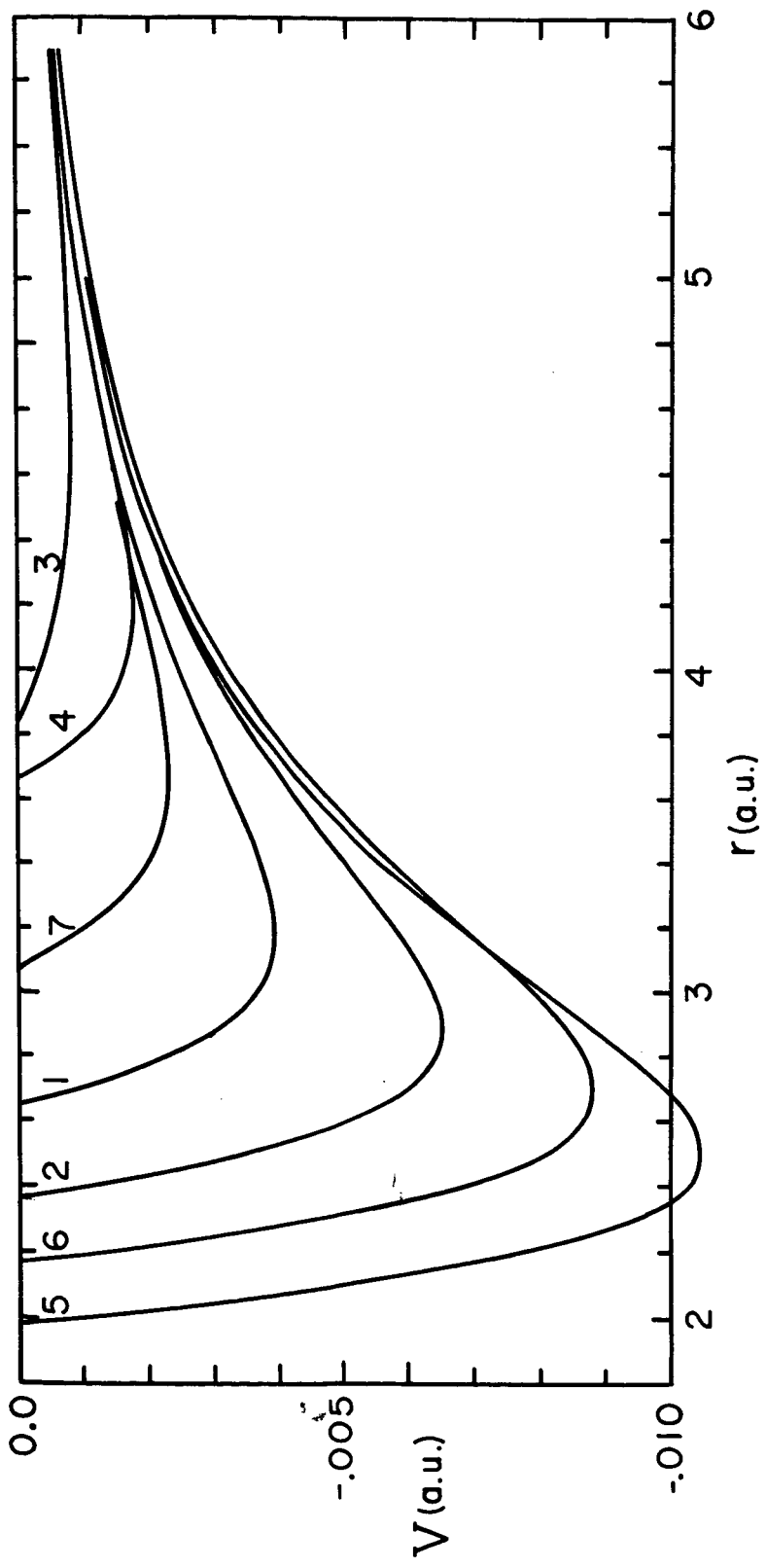


FIG. 1

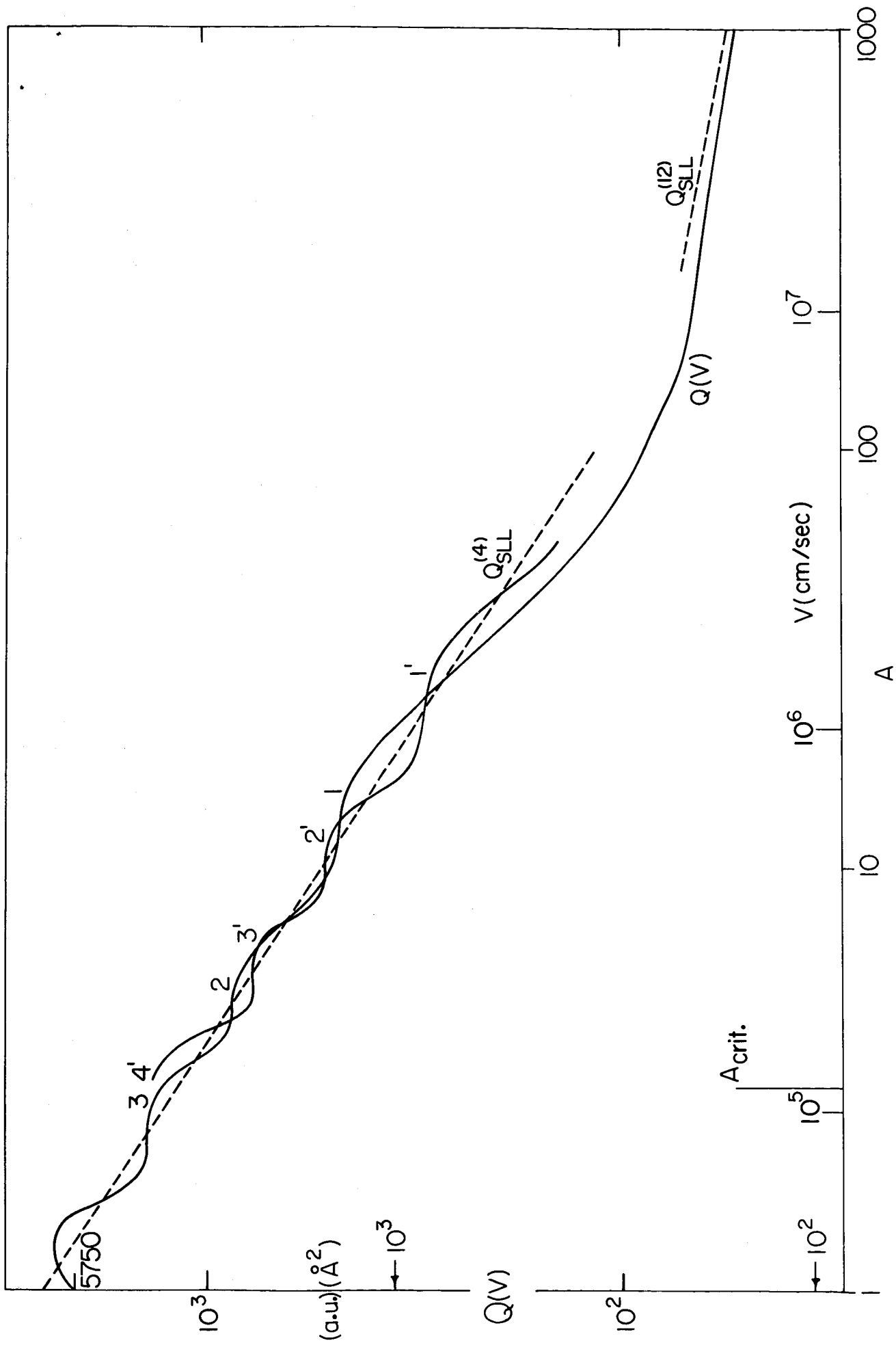


Fig. 2

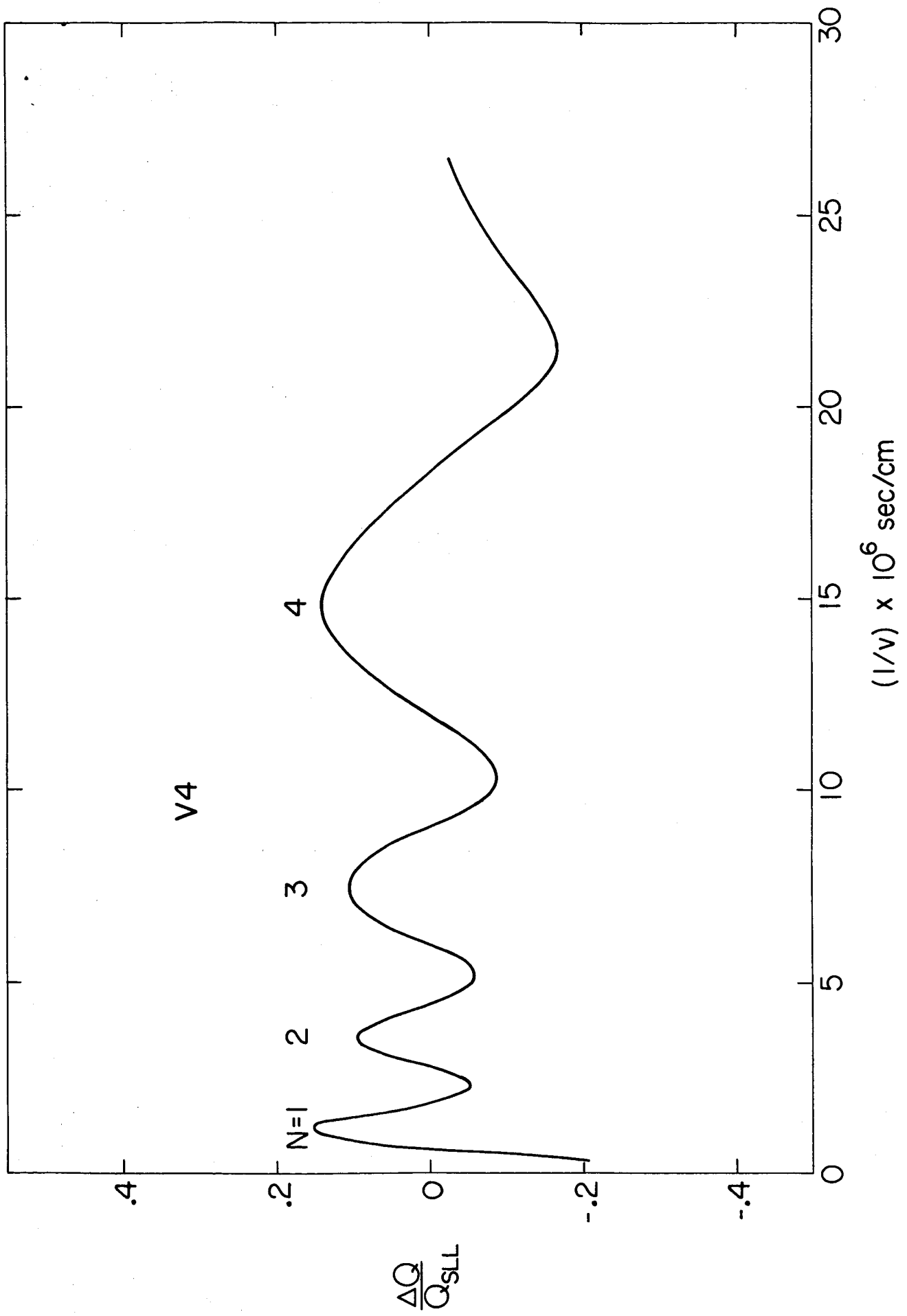


Fig. 3

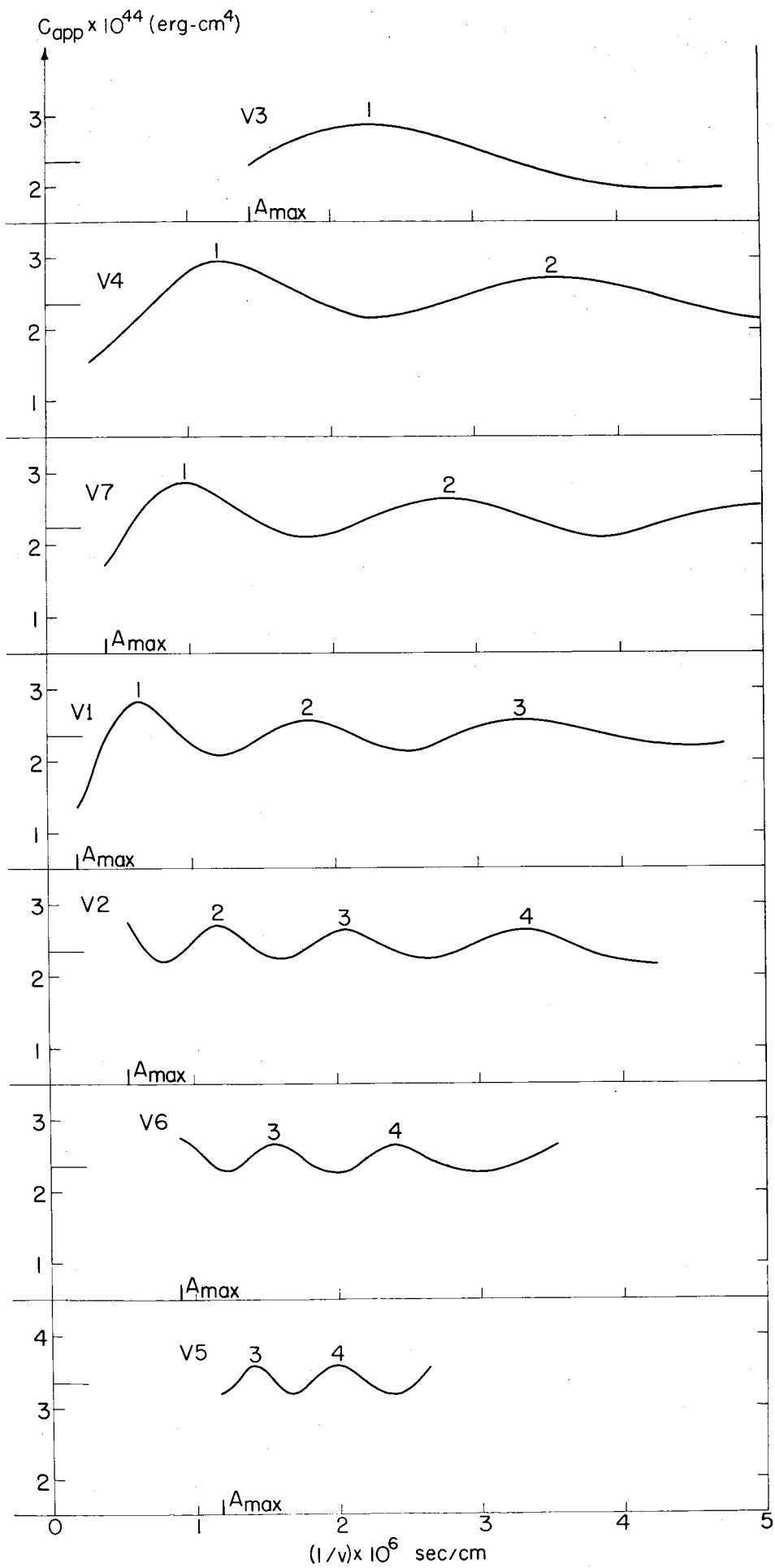


Fig. 4

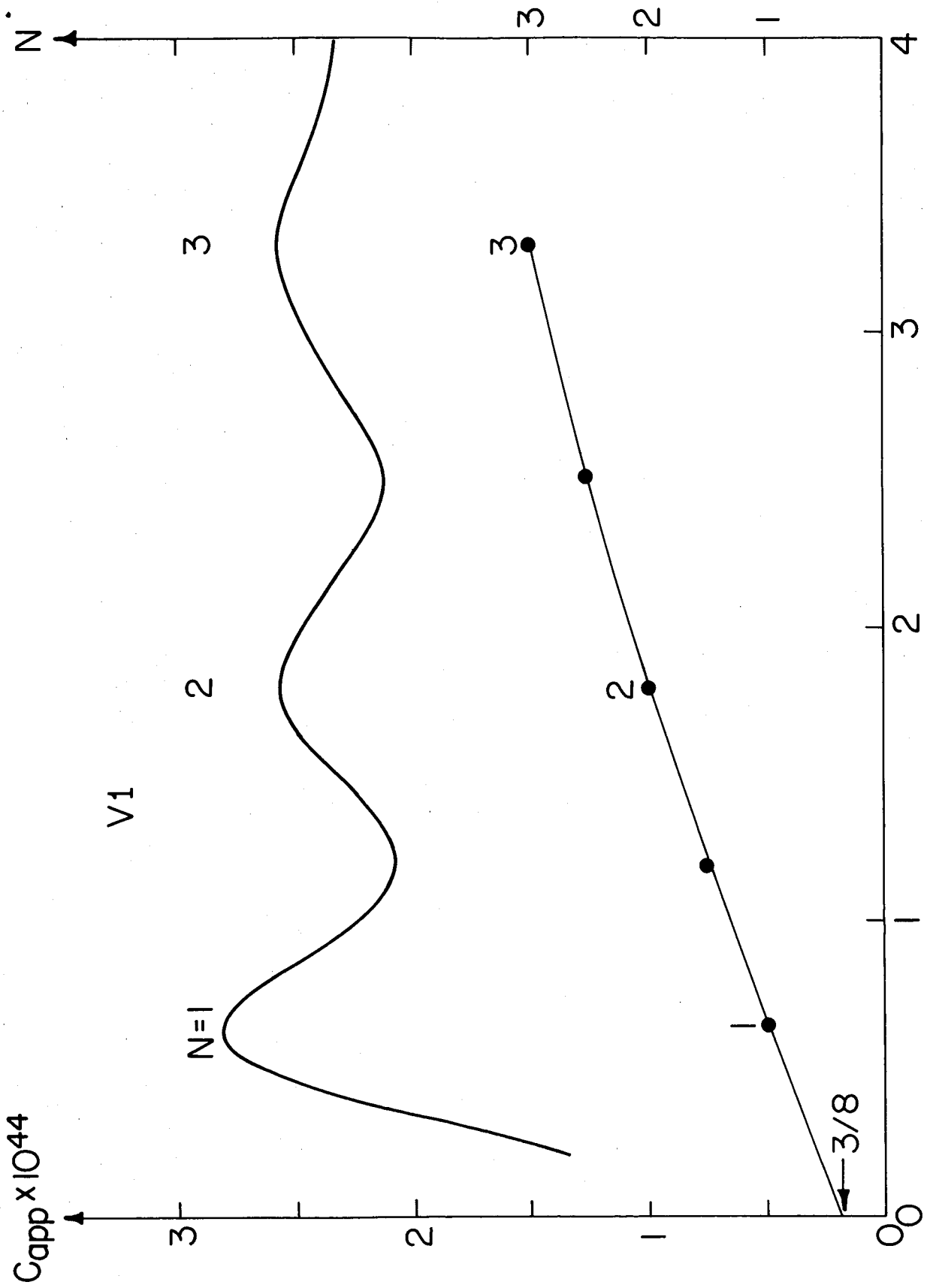
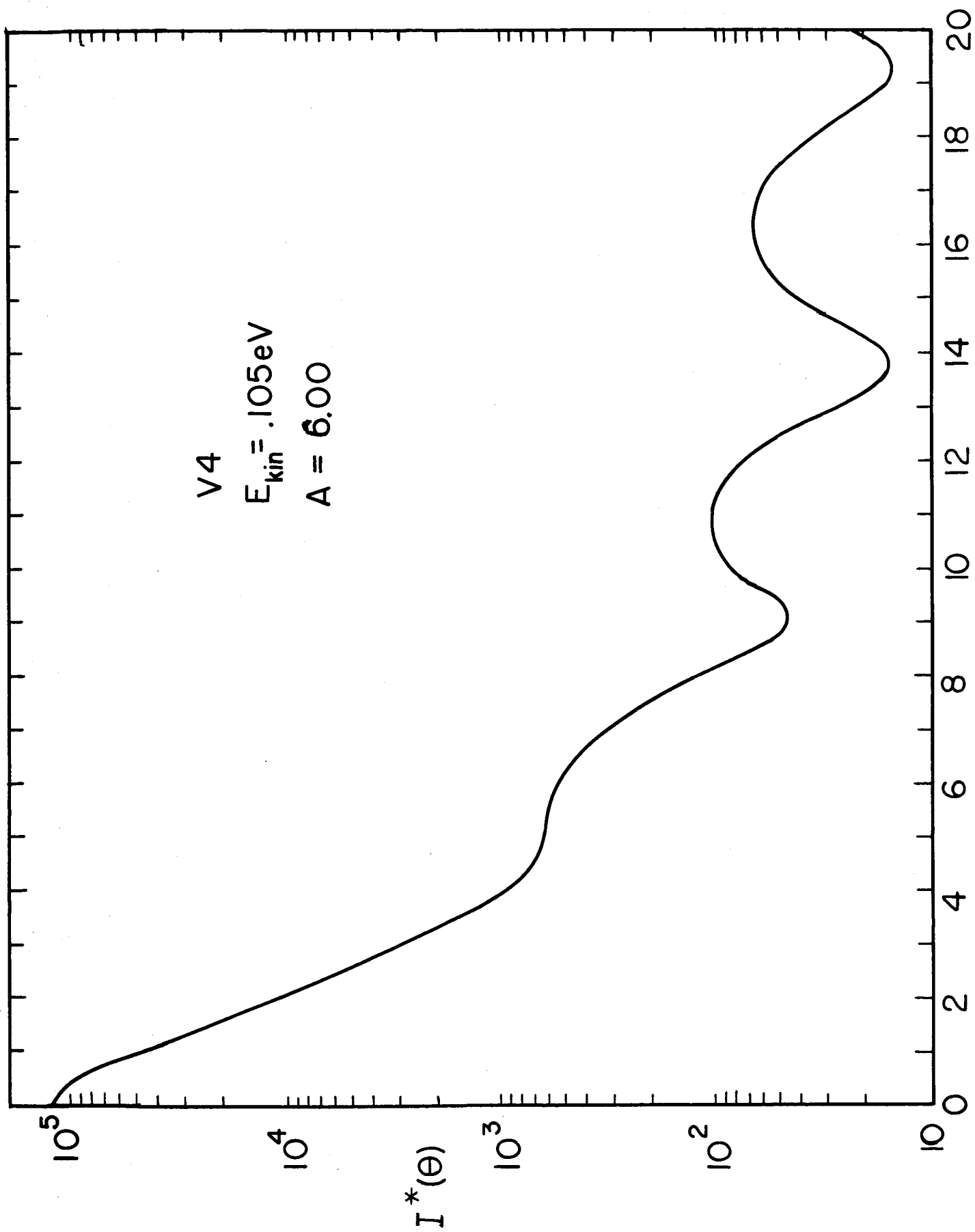


Fig. 5



θ , DEG.

Fig. 6

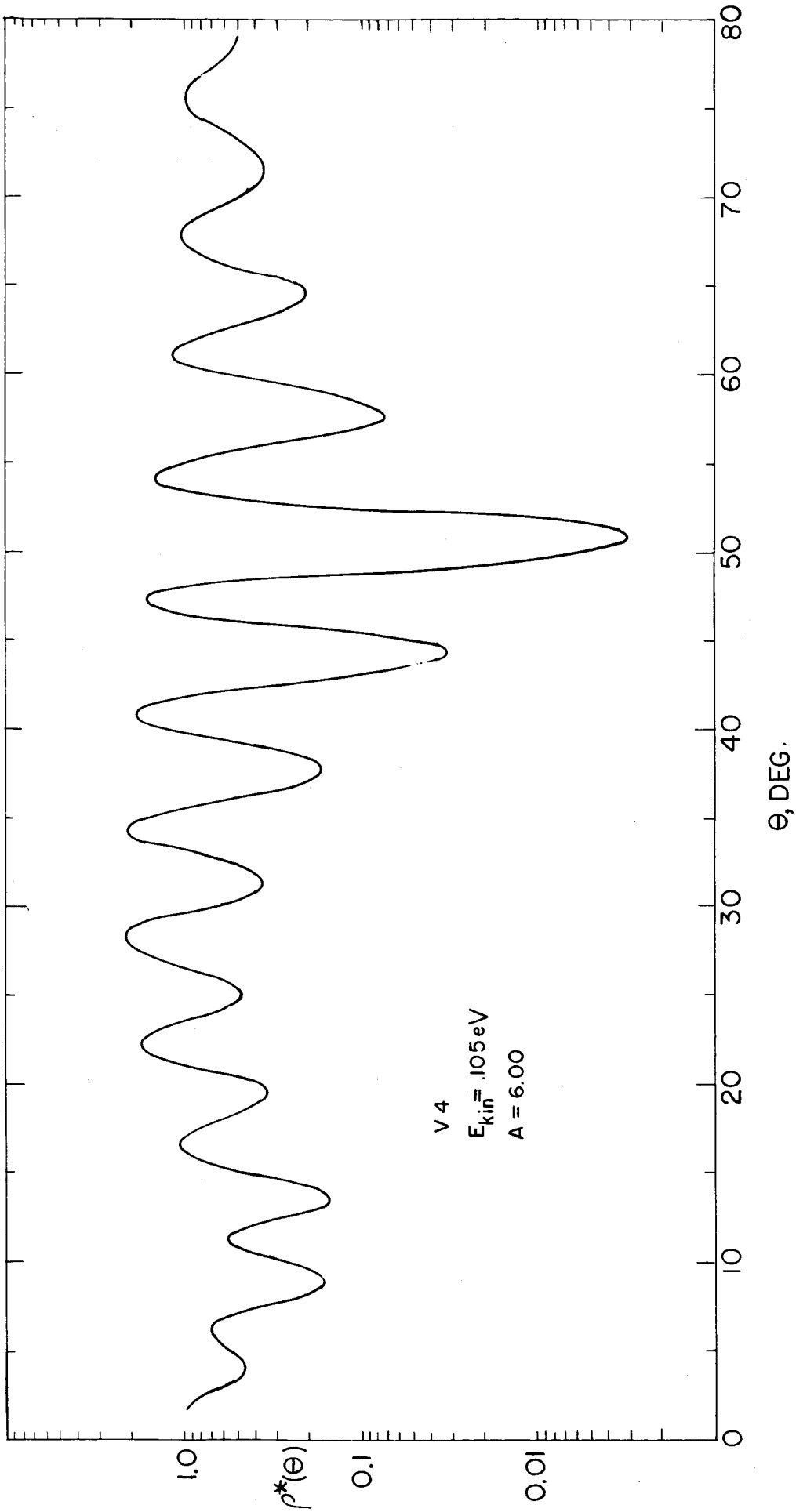


Fig. 7